

Numerical Simulation of a Solar Photovoltaic Panel Cooled by a Forced Air System

D. Nebbali, R. Nebbali, A. Ouibrahim

Abstract—This study focuses on the cooling of a photovoltaic panel (PV). Indeed, the cooling improves the conversion capacity of this one and maintains, under extreme conditions of air temperature, the panel temperature at an appreciable level which avoids the altering. To do this, a fan provides forced circulation of air. Because the fan is supplied by the panel, it is necessary to determine the optimum operating point that unites efficiency of the PV with the consumption of the fan. For this matter, numerical simulations are performed at varying mass flow rates of air, under two extreme air temperatures (50°C, 25°C) and a fixed solar radiation (1000W.m²) in a case of no wind.

Keywords—Energy conversion, efficiency, balance energy, solar cell.

I. INTRODUCTION

MANY studies focuses on the cooled photovoltaic panels. Indeed, the efficiency of such systems is highlighted for hybrid systems as the solar photovoltaic thermal (PV/T), for which the energy consumption required for the air or water circulators are negligible [1]–[3]. To overcome the use of fan circulator, other systems use the cooling by natural circulation of air [4], [5].

The objective of this work is precisely to show that it is possible to cool the PV by forced air. However, an optimum air flow is necessary for a good balance between electric energy generated by the PV and the power consumed by air pump.

Moreover, the upper face of PV is exposed to the external environment where the exchanges take place by natural convection. While, on the underside, the heat exchange by forced convection is ensured by the air flow induced by the fan.

Furthermore, the glass and the silicon layer are the seat of an internal heat source resulting from a heat balance of short and long wave radiations. Numerical simulations are then performed for the case of a monocrystalline PV (0.22m×0.29m×0.025m). The efficiency of the cooling system is compared to the non-cooled one in a case of no wind.

II. A ONE DIODE MODEL

There are several mathematical models that describes the operations and the behavior of the photovoltaic generator, the most famous and classical of them is the one-diode model [6],

D. Nebbali, R. Nebbali and A. Ouibrahim are with the Laboratoire d'Energétique, Mécanique et Matériaux - LEMM (Energy, Mechanics and Materials laboratory), University of Mouloud Mammeri, Tizi-Ouzou 15000, Algeria (e-mail: z_nebbali@yahoo.fr).

[7] which involves: a current generator generated by the illumination, reverse saturation current of the diode associated to the p-n junction and two resistors (series and shunt) for the models that describes the operations and the behavior of the photovoltaic generator, the most famous and classical of them is the one-diode model [6], [7] which involves: a current generator generated by the illumination, reverse saturation current of the diode associated to the p-n junction and two resistors (series and shunt) losses. This model is shown in Fig. 1.

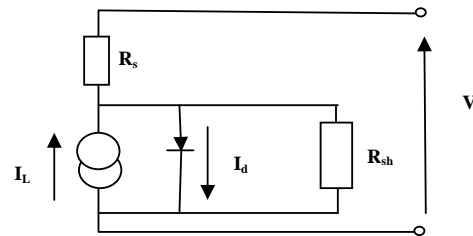


Fig. 1 Equivalent circuit of solar cell (1-diode model)

The analytical formulation of this model is expressed as follow:

$$I = I_L - I_0 \left[\exp\left(\frac{V + IR_s}{a}\right) - 1 \right] \quad (1)$$

A solution of the above equation requires to known five parameters: the light current I_L , the diode reverse saturation current I_0 , the series resistance R_s , the shunt resistance R_{sh} , and a curve fitting parameter a , which are highly related to the intensity of solar radiation and the temperature of the solar panel. These parameters are obtained indirectly using measurements of the current and voltage characteristics of a module at reference conditions (1000 W·m⁻² incident radiation and 25°C ambient air temperature) [8], with the shunt resistance taken as infinity [9]. Under other conditions, it operates the following correlations to evaluate them:

$$a = a_{ref} \frac{T_p}{T_{p,ref}} \quad (2)$$

$$I_L = \frac{R_G}{R_{G,ref}} \left[I_{L,ref} + \mu_{l,cc} (T_p - T_{p,ref}) \right] \quad (3)$$

$$I_0 = I_{0,ref} \left(\frac{T_p}{T_{p,ref}} \right)^3 \exp \left[\frac{\epsilon N_s}{a_{ref}} \left(1 - \frac{T_{p,ref}}{T_p} \right) \right] \quad (4)$$

where

$$I_{L,ref} = I_{cc} \quad (5)$$

$$a_{ref} = \frac{\mu_{V,oc} T_{P,ref} - V_{oc,ref} + \varepsilon N_s}{\frac{\mu_{I,cc} T_{P,ref}}{I_{L,ref}} - 3} \quad (6)$$

and

$\mu_{I,cc} = 1.10^{-4} \text{A} \cdot \text{K}^{-1}$: Temperature coefficient of the short circuit current.

$\mu_{V,oc} = -0.0804 \text{V} \cdot \text{K}^{-1}$: Temperature coefficient of the open circuit voltage.

$\varepsilon = 1.12 \text{eV}$: The band gap energy.

$N_s = 36$: Cells number in series.

In addition, the open circuit voltage V_{co} is expressed by the following relationship [9]:

$$V_{co} = \frac{kT_c}{q} \left(1 + \frac{I_L}{I_0} \right) \quad (7)$$

k : Boltzmann's constant ($\text{J} \cdot \text{K}^{-1}$)

Moreover, the power generated by the solar cell is:

$$P = IV \quad (8)$$

$$P = \left(I_L - I_0 \left[\exp\left(\frac{V + I R_s}{a} \right) - 1 \right] \right) V \quad (9)$$

The maximum electrical power at MPP (P_m) of a module is given by:

$$P_m = V_{opt} I_{opt} \quad (10)$$

where V_{opt} and I_{opt} are respectively the optimum voltage and current.

To evaluate them, it is necessary to solve the following equations:

$$\left. \frac{dP}{dI} \right|_{I=I_{opt}} = 0 \quad (11)$$

The energy efficiency of the solar cell is then defined by:

$$\eta = \frac{P_m}{R_G S} \quad (12)$$

and the absolute efficiency of the installation is:

$$\eta_g = \frac{P_m - P_{fan}}{R_G S} = \eta - \frac{P_{fan}}{R_G S} \quad (13)$$

While the relative efficiency of the installation is expressed by:

$$\eta_r = \frac{\eta_g - \eta_o}{\eta_o} \quad (14)$$

where P_{fan} is the power of the fan and η_o is the efficiency of the PV without cooling system.

III. THERMAL MODEL

A. Heat Balance without Cooling Process

A part of short wave solar radiation (R_G) activates the PV and raises its temperature, while the rest is discharged through long wave radiation and convective heat flux to the ambient air. In the case of no wind, the heat exchanges occur by natural convection on the flat plate of the PV panel.

The heat balance performed at the panel surface (S) can be written as:

$$(R_G S) - \Phi_c - \Phi_r - P = 0 \quad (15)$$

where

Φ_c : the convective heat flux expressed by Newton's law as follows:

$$\Phi_c = hS(T_p - T_{air}) \quad (16)$$

The heat transfer coefficient h is correlated, for the case of a horizontal flat plate under conditions of natural convection, by the following relationship [10]:

$$Nu = 0.54 \times (Ra)^{0.25} \text{ for } 10^4 < Ra < 10^6 \quad (17)$$

$$Nu = 0.15 \times (Ra)^{0.33} \text{ for } 10^6 < Ra < 10^{11} \quad (18)$$

where

Nu : Nusselt number.

$G_r = \frac{\beta g |T_p - T_{air}| L^3}{\nu^2}$: Grashof number

$R_a = G_r P_r$: Rayleigh number.

β : coefficient of thermal expansion (equal to $1/T$ for the ideal gas).

$P_r = \frac{\mu C_p}{\lambda}$: Prandtl number.

$\Phi_r = \sigma S(T_p^4 - T_v^4)$: Net radiation of long wave radiations exchanged between the surface of the PV and the sky.

The temperature of the sky is evaluated by the following relation [11]:

$$T_v = 0.0552 T_{air}^{1.5} \quad (19)$$

TABLE I
MATERIAL PROPERTIES OF PV [12]

Symbol	Quantity	Glass	Silicium
ρ ($\text{kg} \cdot \text{m}^{-3}$)	Density	3000	2330
λ ($\text{W} \cdot \text{m}^{-1} \cdot \text{°C}^{-1}$)	Thermal conductivity	2	130
C_p ($\text{J} \cdot \text{kg}^{-1} \cdot \text{°C}^{-1}$)	Heat capacity	500	677
e (mm)	Thickness	3	0.3

B. Heat Balance with Cooling

1. Governing Equations

The energy balance of heat transfer in the solid media (Silicium and glass, Table I), is given by the Poisson's law:

$$\Delta T + \frac{Q}{\lambda} = 0 \tag{20}$$

where Q is a source term of the net radiative heat of long and short waves, then:

$$Q = R_G S - \varepsilon \sigma (T_p^4 - T_v^4) \tag{21}$$

λ is a thermal conductivity, $\varepsilon=0.7$ is the mean emissivity of the PV's surface while Δ is the Laplace operator.

The heat flux exchanged between the flow air and the wall of the PV panel is determined by solving the equations of continuity, momentum and energy. These equations can be gathered for the case of an incompressible fluid, in the following equation:

$$\frac{\partial \phi}{\partial t} + \nabla \cdot (\phi \vec{V}) = -\gamma \frac{\partial P}{\partial x_i} + \Gamma \Delta \phi \tag{22}$$

wherein the symbols are defined in the table below.

TABLE II
VALUES ASSIGNED TO THE SYMBOLS FOR EACH EQUATION

Symbol	Continuity	Momentum	Energy
Γ	0	ν	α
γ	0	1	0
ϕ	ρ	ρu_i	T

In which $\vec{\nabla}$ is the gradient operator, P the pressure, u_i is the velocity component of vector \vec{V} , ν is the kinematic viscosity, α the thermal diffusivity and T is the temperature.

2. CFD Code

The CFD code Fluent v. 6.1 has been used to perform simulations with the coupling of convective and conductive heat transfers. This code solves the 3D conservation equation energy in solid media with momentum and energy transported by the flow. A fine discretization of the domain studied is used to transform the governing transport equations into a linear equation system solved by the finite volume method.

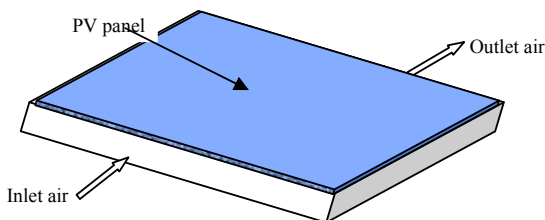


Fig. 2 Domain model with boundary conditions

IV. RESULTS

It appears in Fig. 3 that the temperature of the PV decreases with the increase of the air mass flow rate. Indeed, the velocity of the fluid increases and improves the convective heat exchange between the air and the inner surface of the PV. Beyond a flow of $30 \text{ g} \cdot \text{s}^{-1}$, the temperature of the PV decreases weakly and tends to the inlet air temperature.

However, this flow rate value is not recommended for optimum operation of a PV. Indeed, an increase in throughput is concomitant to an increase a fan's energy consumption (Fig. 4).

As shown in Figs. 5 and 6, the global efficiency of the system increases up to a maximum value corresponding to a flow rate value of $8 \text{ g} \cdot \text{s}^{-1}$, above which it begins to decrease.

This flow rate is the optimum functioning value of the PV. The PV panel is cooled until 41°C and 63°C , respectively, for the outdoor air temperatures of 25°C and 50°C (Fig. 3).

Under these temperature conditions, the characteristics curves of the PV take the shapes shown in Figs. 7 and 8.

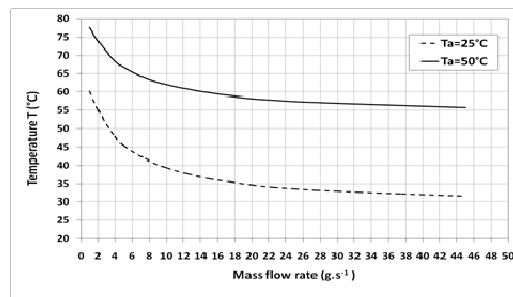


Fig. 3 Evolution of the PV temperature with the mass air flow for Ta=25 and 50°C

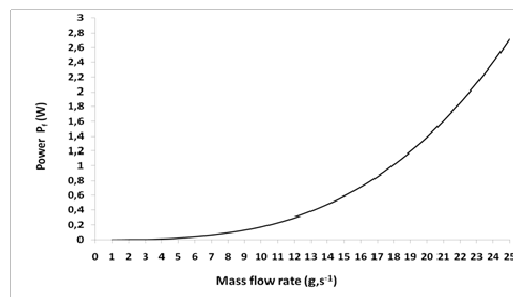


Fig. 4 Characteristic curve of the fan

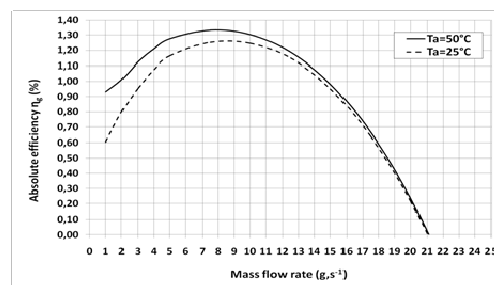


Fig. 5 Absolute efficiency of the system as a function of mass air flow

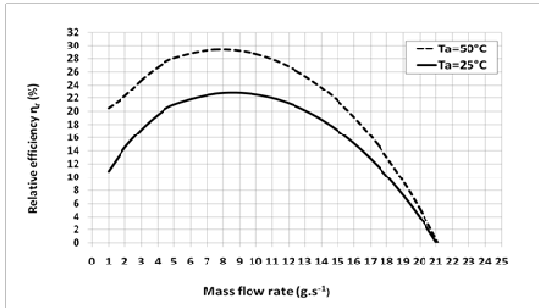


Fig. 6 Relative efficiency of the system as a function of mass flow rate

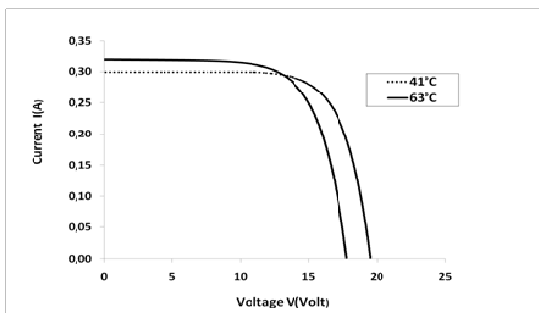


Fig. 7 Characteristic curve of PV at the temperatures $T_p = 41$ and 63°C

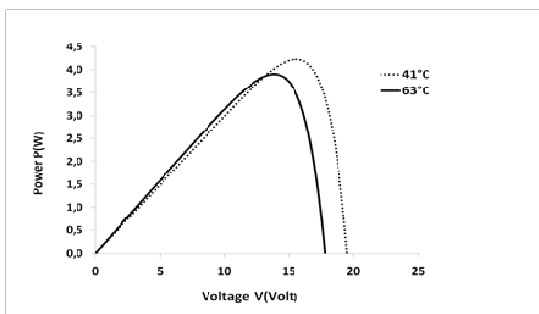


Fig. 8 Evolution of the power of the PV at the temperatures $T_p=41$ and 63°C

V. CONCLUSION

The influence of both solar radiation and temperature leads to the necessary use of an electrical model. Thus, on a first step, we begin to manage a one-diode electrical model.

Furthermore, in the case of no wind and without cooling system, the temperature of the PV is determined by a heat balance which includes both radiatives (short and long wavelengths) and convective exchanges. The equations obtained are then solved by successive iterations.

For the case of a PV cooled by a forced air, we use a CFD code to solve the coupled equations of continuity, motions and energy in different media. We highlight that the increase of mass flow rate, concomitant to the power consumed by of the fan, decreases the PV's temperature. Taking into account the characteristic curve of the fan, we show the influence of the

air mass flow rates on the overall efficiency of the installation.

However, the optimum value of the mass flow rate is obtained at $8\text{ g}\cdot\text{s}^{-1}$ which ensures a mean temperature of 41 and 63°C for the PV, respectively, for 25 and 50°C of air temperature. At this optimum, the growth of the absolute efficiency is 1.25 and 1.35% , while the growth of the relative efficiency is 23 and 29% for each case.

REFERENCES

- [1] F. Sarhaddi, S. Farahat, H. Ajam, A. Behzadmehr and M. MahdaviAdeli, "An improved thermal and electrical model for a solar photovoltaic thermal (PV/T) air collector," *Applied Energy*, vol. 87, 2010, pp. 2328–2339.
- [2] A. Tiwari and MS. Sodha, «Performance evaluation of solar PV/T system: an experimental validation," *Solar energy*, Vol. 80, July 2006, pp. 751–759.
- [3] S. Armstrong and W.G. Hurley, "A thermal model for photovoltaic panels under varying atmospheric conditions," *Applied Thermal Engineering*, vol. 30, 2010, pp.1488–1495.
- [4] E. Skoplaki and J.A. playvos, "On the temperature dependance of photovoltaic module electrical performance: A review of efficiency/power correlations," *Solar Energy*, vol. 83, 2009, pp. 614–624.
- [5] H.G. Teo, P.S. Lee and M.N.A. Hawlader, "An active cooling system for photovoltaic modules," *Applied Energy* 90, vol. 1, 2011, pp. 309–315.
- [6] D.L. King, W.E. Boyson and J.A. Kratochvil, "Photovoltaïque array performance model," New Mexico: Photovoltaic system R&D Department, Sandia National Laboratories, P.O. Box 5800, Albuquerque, August 2004.
- [7] W. DeSoto, S.A. Klein and W.A. Beckman, "Improvement and validation of a model for photovoltaic array performance," *Solar Energy*, vol.80, 2006, pp. 78–88.
- [8] T.U. Townsend, "A Method for Estimating the Long Term Performance of Characteristics of Solar Cells," *Solar Cells*, Vol. 4, N°2, 1981, pp. 169–178.
- [9] John A. Duffie, William A. Beckman, "Solar Engineering Of Thermal Processes," New York: University of Wisconsin-Madison, 1988, pp. 270–280.
- [10] J. P. Holman, "Heat Transfer," 8th edition, McGraw-Hill, 1997.
- [11] J. I. Montero, A. Muñoz, A. Antón and N. Iglesias, "Computational fluid dynamic modelling of night-time energy fluxes in unheated greenhouses," *Acta Horticulturae*, Vol. 691, 2004, pp. 403–410.
- [12] M.U. Siddiqui and A.F. Arif, "Electrical, thermal and structural performance of a cooled PV module: Transient analysis using a multiphysics model," *Applied energy*, vol. 112, 2013, pp. 300–312.